Frontiers in Magnetism
J. Phys. Soc. Jpn. **69** (2000) Suppl. A. pp. 297–302

High-Field, High-Frequency ESR in the One-Dimensional Quantum Spin Systems

Yoshitami AJIRO[1], Takayuki ASANO[1], Yuji INAGAKI[1], Jean-Paul BOUCHER[1,2], Hiroyuki NOJIRI[3], Sebastian LUTHER[3], Takuo SAKON[3], Mitsuhiro MOTOKAWA[3],

[1]*Department of Physics, Kyushu University, Fukuoka 812-8581, Japan*
[2]*Laboratoire de Spectrométrie Physique, Université Joseph Fourier, BP 87, F-38402 Saint-Martin d'Hères Cedex, France*
[3]*Institute for Materials Research, Tohoku University, Sendai 980-8577, Japan*

(Received February 1, 2000)

We applied the high-field, high-frequency electron spin resonance (ESR) technique to study the field-dependent behaviors of three representative examples of quantum spin chain. (1) In the half-integer ($S = 1/2$) antiferromagnet Cu-benzoate, $Cu(C_6H_5COO)_2 \bullet 3H_2O$, we observed rather unusual temperature- and field-dependences of the shift and width of the resonance line. These results are discussed in terms of the breather excitations predicted by Oshikawa and Affleck for this compound. (2) For the integer ($S = 1$) antiferromagnet NDMAZ, $Ni(C_5H_{14}N_2)_2N_3(ClO_4)$, we observed various ESR modes both in the nonmagnetic Haldane phase ($H < H_c$) and in the magnetic high-field phase ($H > H_c$) where H_c is the critical field at which the Haldane gap closes. From the frequency-field diagram and the temperature dependence of the signal intensity, we discuss the possible origin of these ESR modes. (3) For $S = 1/2$ trimerized chain, $3CuCl_2 \bullet 2$dioxane, we observed unique features of a composite spin system, such as a dynamical process of the formation of $S = 3/2$ trimerized units from three $S = 1/2$ spins, as indicated by the signal splitting into 3 lines at most depending on the frequency and gradual change of the resonance fields with decreasing temperature.

KEYWORDS: high-field, high-frequency, ESR, one-dimensional, quantum-spin

§1. Introduction

Quantum antiferromagnetism in low dimensional systems has been a subject of intense study in recent years. Electron spin resonance (ESR) is a particularly sensitive technique to probe characteristic low energy excitations. In this seminar paper, we review our recent results of a high-frequency and high-field ESR study on three representative examples of quantum spin chains, performed at low temperatures by combining pulsed magnetic fields up to 30 T with radiation sources up to 1000 GHz.

§2. Half-integer ($S = 1/2$) quantum spin chain, Cu-benzoate

Cu-benzoate, $Cu(C_6H_5COO)_2 \bullet 3H_2O$, has been considered as a good representative of $S = 1/2$ Heisenberg quantum spin chain (HQSC) with an antiferromagnetic coupling $J = 8.6$ K.[1] Recent intensive measurements of specific heat and neutron scattering, however, revealed rather unusual features of magnetic excitations under the external field below 1 K.[2,3] Besides the dynamical incommensurability expected for HQSC in high magnetic fields, an unexpected field-induced energy gap $E_G(H) \propto H^{2/3}$ in the magnetic excitation spectrum was observed at low temperature. It should be noted that no three-dimensional (3D) magnetic ordering was found in above measurements down to 0.1 K and thus the observed features should be attributed purely to the one-dimensional and dynamical character of the system. Based on a field theoretical approach, a description was then proposed by Oshikawa and Affleck (OA)[4,5] and, subsequently by Essler and Tsvelik.[6,7] They claimed that the field-induced gap is caused by the effective staggered magnetic field acting between neighboring spins in the chains and has a non-trivial power dependence $H^{2/3}$ on the applied field H in agreement with the experiments. It is rather well known from a general argument based on the crystal symmetry that the staggered field, being perpendicular and proportional to the applied uniform field, is produced by the alternating g-tensor and the Dzyaloshinsky-Moriya (DM) interaction in some crystal symmetry.[8] Most importantly, the HQSC system subjected to the perpendicular staggered field is well described by a quantum sine-Gordon model on the basis of a low energy effective field theory. The quantum sine-Gordon model is exactly solvable and, in particular, its elementary excitation is known to consist of soliton, antisoliton and their bound states which are called "breathers".

The anomalies of the magnetic excitation were previously observed in the ESR measurements at low temperature by Oshima *et al.* more than 20 years ago.[9] Although their explanation for the low temperature ESR signals as the manifestation of the 3D ordering was not compatible with the most recent results, their results are recently reanalyzed in terms of the newly proposed breather excitation.[10] On the basis of the sine-Goldon model, it is shown that the ESR intensity is dominated by the breather mode in the extremely low temperature limit. This theoretical approach of ESR is, however, restricted to low field ($H \ll J$) and low temperature ($T \ll J$). In order to examine the predicted behaviors and what happens in the high field limit, we extended the ESR measurements to a sufficiently high field range comparable or much larger than the exchange coupling, i.e., $H > J$. If this picture can be applied to the real system of Cu-benzoate, the anomalies of the ESR signals should appear in the similar manner as observed by Oshima *et al.* even in relatively higher temperatures when the condition $T \ll E_G(H)$ is satisfied in high magnetic fields. Thus it is very important to perform the ESR measurements in the wide field and temperature ranges by using the advanced technique of high frequency ESR developed in these several years.

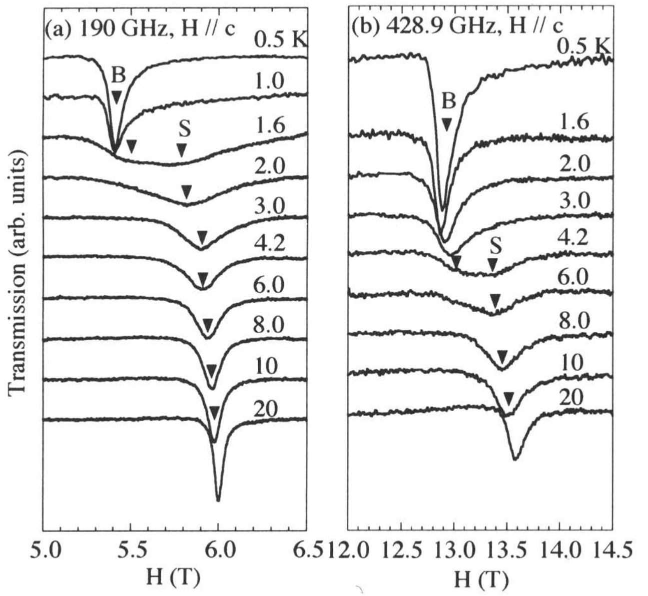

Fig. 1. Examples of ESR spectra at (a) 190 GHz and at (b) 428.9 GHz for $H \| c$. The closed triangles represent spinon ESR signal (S) and first-breather ESR signal (B).

We observed rather unusual behaviors of ESR spectra as a function of temperature and frequency. As shown in Fig. 1, the signal S shifts to the lower field side with decreasing the temperature when $T \leq J$, accompanied with the rapid broadening of the line width. As the temperature is decreased further, a novel crossover takes place as indicated by a double-peak structure at the crossover regime ($T \sim E_G(H)$). While the width of the signal S increases continuously, the integrated intensity of this signal decreases gradually. At the same time, the new signal B appears in the low field side. The signals S and B coexist in some temperature region, and, in this crossover regime, the spectral weight shifts gradually from the signal S to the signal B. At the lowest temperature ($T < E_G(H)$), finally the absorption intensity of the signal B becomes dominant. Of particular interest is that the crossover regime depends on the frequency and, consequently, on the field, as easily seen from the comparison between (a) 190 GHz data and (b) 428.9 GHz data. In fact, the crossover appears when the temperature is comparable to the field-induced gap. Since the magnitude of the energy gap changes as $E_G(H) \propto H^{2/3}$, this crossover temperature also depends on the magnetic field intensity as $H^{2/3}$. This finding clearly indicates that the crossover regime designates the boundary between the gapless high T-low H state ($E_G(H)/T < 1$) and the gapped low T-high H state ($E_G(H)/T > 1$). The drastic change of the ESR spectra is usually considered to be an indication of onset of the 3D ordering but it is not the case for Cu-benzoate. The anomaly can be explained in terms of the dynamical crossover between the gap-less "spinon" regime and the gapped "breather" regime. For a HQSC, a gapless spinon excitation develops due to the short-range correlation within the spin chains when a temperature is much lower than J. In this spinon regime, a drastic broadening of the ESR line width is caused by a staggered field due to development of the correlation length.[10] Actually, for $E_G(H)/T < 1$, the theoretically predicted $(H/T)^2$ dependence of the linewidth features well both the temperature and field dependences of the linewidth of the signal S at different frequencies. In the gapped regime, it is theoretically proposed that the ESR intensity is dominated by the breather excitations. Indeed, for $E_G(H)/T > 1$, we observed a new signal B corresponding to the characteristic excitations in the gapped state.

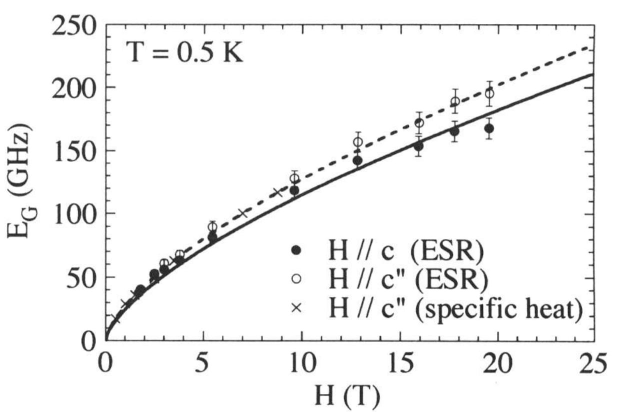

Fig. 2. The plot of $E_G(H)$ as a function of external field. The closed and open circles represent the values obtained by the present work. The crosses show the value determined by the specific-heat measurements taken from Ref.[3]

In order to confirm that the signal B is certainly the breather mode, we examined the frequency-field dependence of the signal B at 0.5 K for different field orientations. The resonance field shifts to the low field side from the conventional Zeeman mode and its frequency-field curve exhibits the nonlinear field dependence, reflecting the existence of the energy gap whose magnitude depends on the field orientation in accordance with the angular dependence of the field-induced gap. All these observations, including the temperature and field-dependences of the linewidth are consistent with the predicted behaviors.[10] According to OA, the ESR frequency-field relation of the breather mode is given by

$$h\nu = \sqrt{(g\mu_B H)^2 + E_G(H)^2}, \tag{2.1}$$

where ν and g are the frequency of ESR and the g-value, respectively. From this relation, we can determine the $E_G(H)$ straightforwardly by putting the experimental values of ν, H and g. The results are shown in Fig. 2, together with the predicted field dependence $H^{2/3}$. Now it is evident that the signal B is characteristic of the predicted breather mode and it is surprising that the eq. (2.1) is valid in the wide field range including a high field condition as $g\mu_B H > 2J$. Some of the results[11] and more details[12] will be published elsewhere.

§3. Integer ($S = 1$) antiferromagnet, NDMAZ

The ground state of Heisenberg antiferromagnetic chains of integer spins is nonmagnetic.[13] The low-energy triplet excitation displays a quantum Haldane gap E_G above the singlet ground state. These features have been established experimentally, first in NENP [$Ni(C_2H_8N_2)NO_2(ClO_4)$].[14-16] Numerous ESR investigations[17-20] have been performed on this prototypical compound NENP. After some confusion, the observed resonances are now interpreted as follows. Below the critical field H_c, at which the spin gap closes, there exist two kinds of resonances designated as high- and low-frequency ESR modes, corresponding to the transitions between the triplet magnon excitations (at $q = \pi$) and to those induced from the ground state (at $q = 0$). The latter resonances are nominally forbidden by selection rules for ESR transitions, though it is considered that they are allowed in NENP due to the existence of a staggered g-tensor.[21,22] Much less is known about the ESR transitions, especially high-frequency modes, in the magnetic high-field phase above H_c. For $H > H_c$ the system is expected to be gapless when the staggered term is absent. The staggered term lifts the degeneracy between the magnetic ground state and the first excited state in the high field phase yielding a gap which increases with H, as examined recently by intense study of the low-frequency ESR mode.[23]

In view of such complexity in the signal assignment, it is certainly necessary to push the ESR measurements to a much simpler system which has no staggered g-tensor. In the present work, measurements are performed on the single crystal of the new Haldane system, NDMAZ [$Ni(C_5H_{14}N_2)_2N_3(ClO_4)$] which displays a Haldane gap of ~20 K and has no staggered g-tensor.[24] Various ESR lines were observed below and above H_c. Figure 3 shows the frequency-field diagram of the ESR signals at 1.6 K, 4.2 K and 6.0 K, for three perpendicular field directions along the a^*, b and c axes where c is parallel to the chain axis. At the first glance, all signals are observed rather continuously as a function of the external field. However, a distinction is to be made between those signals below and above the critical field H_c. Here, we note that H_c is angular dependent and is known to be 20 T for $H\|a^*$, 18 T for $H\|b$, and 12 T for $H\|c$, respectively.

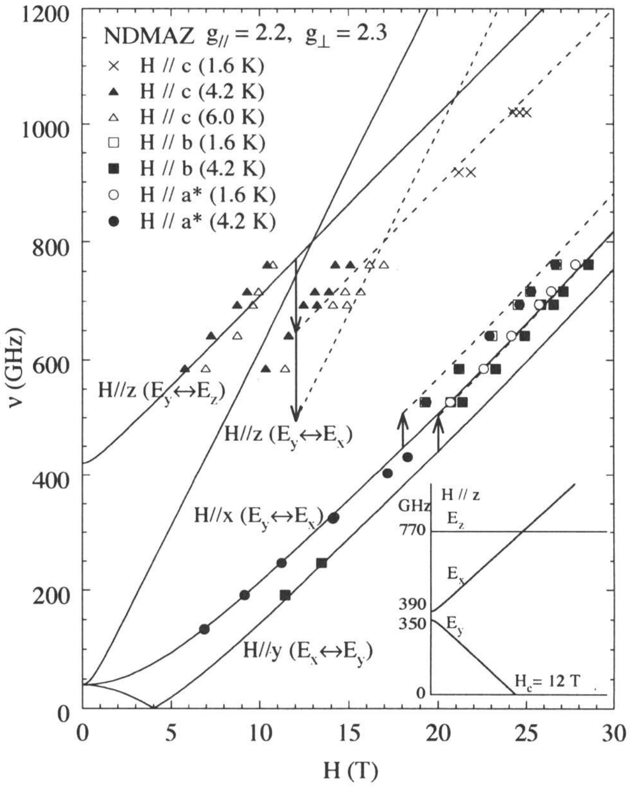

Fig. 3. The frequency field diagram of the ESR signals at 1.6, 4.2 and 6.0 K, for three field directions along the a^*, b and c axes where c is parallel to the chain axes. The solid lines are the calculated results for $H\|x$, y and z, based on the energy levels in the inset.

All the signals below H_c are weaker than those observed above H_c. Moreover, their intensity decreases with decreasing temperature, indicating that they are induced from excited triplet states. Accordingly, they can be attributed to transitions between the triplet excited states. It is noteworthy that the low-frequency mode induced from the singlet ground state is missing contrary to the case of NENP, in agreement with the absence of a staggered g-factor.

Above H_c, the signal intensity increases with decreasing temperature, indicating that they are induced from the ground state. It is remarkable that all the other striking features of the high-frequency modes such as shifts of the resonance field towards lower fields and the occurrence of a sharp fine structure with decreasing temperature are common to those observed previously in NENP. Therefore, it is now clear that these features characterize the high-frequency ESR modes in the high field phase, irrespective of the existence of the staggered field.

To analyze the frequency-field diagram, we use the energy levels proposed by Tsvelik.[25] To account explicitly for the presence of the single-ion anisotropies D and E, we introduce three distinct gaps at zero field, as Δ_x, Δ_y

and Δ_z, between the ground state and the excited triplet states at $q = \pi$. The energy levels of triplet states for $H\|z$ are given by

$$E_x(H) = \frac{\Delta_x + \Delta_y}{2} + \sqrt{(g_\| \mu_B H)^2 + \left(\frac{\Delta_x - \Delta_y}{2}\right)^2},$$
$$E_y(H) = \frac{\Delta_x + \Delta_y}{2} - \sqrt{(g_\| \mu_B H)^2 + \left(\frac{\Delta_x - \Delta_y}{2}\right)^2},$$
$$E_z(H) = \Delta_z. \tag{3.1}$$

For H applied in another direction, the same expression can be used, after a circular permutation is performed in the indices x, y and z. The inset of Fig. 3 shows the calculated energy diagram for $H\|z$, as an example, using the values of $\Delta_x = 390$ GHz, $\Delta_y = 350$ GHz, $\Delta_z = 770$ GHz and $g_\| = 2.2$. Important spin-Hamiltonian parameters J, D and E can be deduced from these gaps; that is, $0.41J = E_G = (\Delta_x+\Delta_y+\Delta_z)/3$, $D = (\Delta_x+\Delta_y)/2-\Delta_z$ and $E = (\Delta_x-\Delta_y)/2$. The solid lines in Fig. 3 represent the calculated frequency-field diagrams for the respective directions. Below H_c, the agreement with the experimental data are satisfactory for all directions except close to H_c along the z axis. The deviation is, however, likely to be explained in terms of a possible crossover effect due to the level repulsion near the level-crossing point.

We now turn to the discussion of the high-frequency modes above H_c. Contrary with the modes below H_c, a remarkable discrepancy to the smoothly extrapolated curves from low field phase can be seen for all the modes above H_c. At the same time, however, it should be noted that a deviation from the extrapolation curves is almost constant.

Although no definite interpretation for the high-frequency modes of the high-field phase is known at present, this parallel deviation tempts us to simply introduce some bias field to explain a constant shift above H_c. The trial curves, assuming the traceless bias field ($H_x = 2$ T, $H_y = 2$ T and $H_z = -4$ T) for respective axes, are shown by the broken lines. It is worth mentioning that the existing data for high-field phase in NENP can be also consistently interpreted by introducing a bias field mentioned above. If this is a case, it suggests that a character of the triplet magnon excitations may not change so much at H_c as far as the field-dependent energy diagram is concerned, though the ground state above H_c is quite different from the nonmagnetic singlet state below H_c. Much less is known about the ground state excitations above H_c and, thus, more experimental and theoretical investigations are certainly required to extend the knowledge about the high field phase in the Haldane systems.

§4. $S = 1/2$ trimerized chain, $3CuCl_2$•2dioxane

An interesting third example is a composite spin system, $3CuCl_2$•2dioxane ($C_4H_8O_2$), in which ferromagnetic trimers consisting of three $S = 1/2$ spins are weakly coupled antiferromagnetically in one dimension. A trimer has the $S = 3/2$ ground state due to a strong intratrimer ferromagnetic interaction. Thus, the system can be approximated by an $S = 3/2$ antiferromagnetic chain at low temperatures. High field magnetization at 1.5 K increases nonlinearly and saturates around $H_s = 15$ T. The magnetization data show a remarkable spin reduction, suggesting that a composite spin system consisting of three $S = 1/2$ spins has more of a quantum nature than does a genuine $S = 3/2$ system.[26]

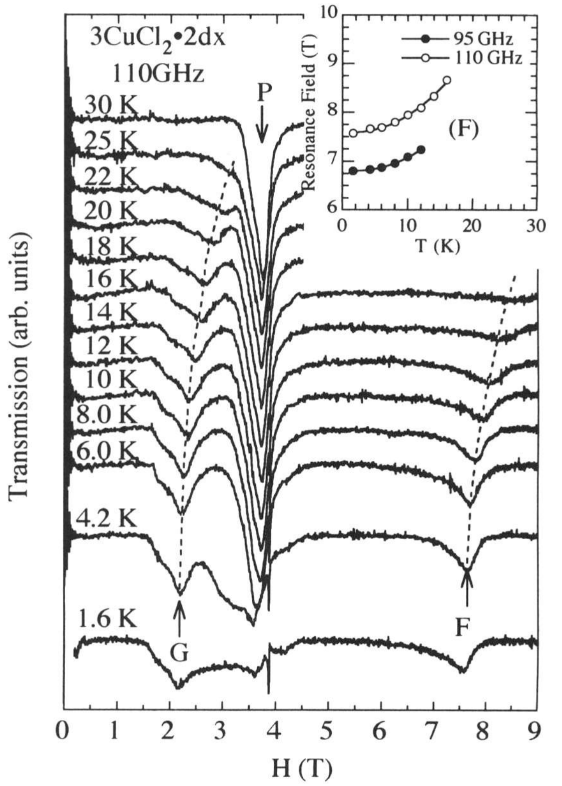

Fig. 4. Typical example of the ESR spectra at 110 GHz. The inset shows the temperature dependence of the resonance field of the signal F.

Figure 4 shows the typical example of the ESR spectra at 110 GHz. At high temperatures, a single paramagnetic signal P typical for Cu^{2+} ions is observed but ESR spectrum splits into 3 lines at most, depending on the frequency as the temperature decreases. Below about 30 K a new signal G grows up at the low field side of the signal P with a gradual change of the resonance field. As the temperature decreases further below about 20 K, another new signal F appears at a quite different field. As easily seen in the inset of Fig. 4, the resonance field of the signal F rises more and more rapidly to the higher field and the effective g-values, defined as $g_{\text{eff}} = h\nu/\mu_B H$, decreases toward zero as the temperature approaches to 30 K like a compensation point in ferrimagnets.

Figure 5 shows the frequency-field diagram at 1.6 K for these signals. It displays clearly the existence of a characteristic gapped mode G with a finite energy gap $\Delta = 92$ GHz at zero field. This signal merges at around 150 GHz into the paramagnetic branch P on the straight line with a slope $g = 2.2$ starting from the origin. In ad-

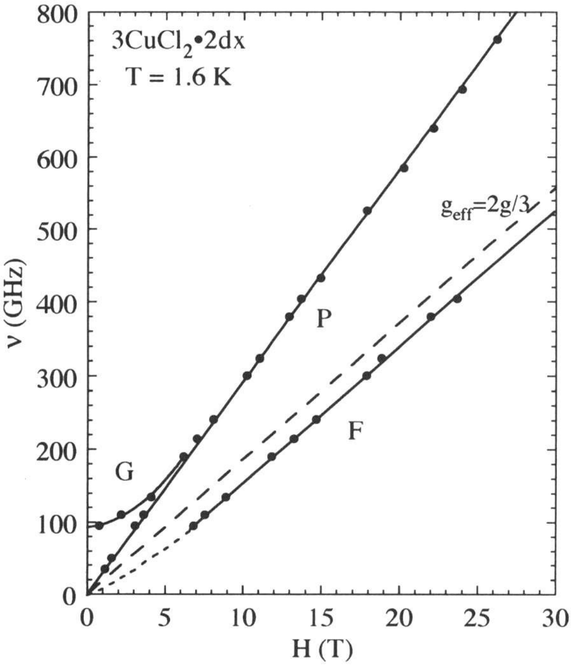

Fig. 5. The frequency-field diagram at 1.6 K. Three branches P, G and F are designated.

dition, we see the ferrimagnetic branch F on the straight line with a slope $2g/3 = 1.47$ and we naively speculate that the branch F continues smoothly toward zero at lower frequency, as indicated by the broken line. The characteristics of the signal F are very peculiar in the sense that g_{eff} decreases toward zero both at about 30 K as a function of temperature and at low frequency as a function of frequency or field, and has a fractional g-value at low temperature and high frequency. The reason why we named the F signal as the ferrimagnetic mode is due to these peculiarities. The mentioned characteristics resemble somewhat to the well-known ferrimagnetic resonance.[27] According to the general theory of the ferrimagnetic resonance, the solution of equations of motion for two coupled magnetic moments M_{A} and M_{B} leads us to the following resonance equation,

$$h\nu = g_{\text{eff}}\mu_{\text{B}}H, \tag{4.1}$$

where

$$g_{\text{eff}} = g\left(1 - |M_{\text{B}}|/|M_{\text{A}}|\right), \tag{4.2}$$

when the natural relaxation of M_{A} is neglected and the rapid relaxation of M_{B} is assumed. It should be stressed that the above equation is not derived from the simple ferrimagnetic model with stable sublattice magnetization with same g-values and is applicable only for the dynamical condition that M_{B} relaxes very rapidly. Interestingly enough, this equation naturally explains the observed peculiarities of the temperature and frequency dependences of g-value: g_{eff} is changeable from zero for $|M_{\text{B}}/M_{\text{A}}| = 1$ to g for $|M_{\text{B}}/M_{\text{A}}| = 0$, allowing the fractional value $2g/3$ for $|M_{\text{B}}/M_{\text{A}}| = 1/3$.

Now let us discuss the physical scenario of the above observations. According to the theoretical calculation at $T = 0$,[28] the magnetization curve will exhibit the so called 1/3 plateau when the intratrimer ferromagnetic interaction J_{F} is not much stronger than intertrimer antiferromagnetic interaction J_{AF}, that is, for the ratio of $\gamma = J_{\text{F}}/J_{\text{AF}}$ less than about 3. It does mean the existence of the intermediate state of $S = 1/2$ with the energy gap. It should be noted that this state is more favorable in the finite system and in the finite field. At a temperature much higher than J_{F}, the system behaves simply as a collection of the paramagnetic $S = 1/2$ spins, resulting in a normal ESR signal P which is exchange-narrowed by J_{F} and J_{AF}. With decreasing temperature, however, the short range correlations develop within the ferromagnetic trimers due to J_{F} and also between the trimers due to J_{AF}. In this circumstance, we imagine the local magnetic cluster with finite length and expect the relatively stable $S = 3/2$ entity and the less stable $S = 1/2$ entity for the condition of $J_{\text{F}} > J_{\text{AF}}$. This $S = 1/2$ entity just corresponds to the intermediate state at $T = 0$ mentioned above. Although 1/3 plateau was not observed in the present case with $\gamma = 5$, we still expect the existence of the excited state of $S = 1/2$ with the finite energy gap and finite life time. From this scenario, it is easy to identify the origin of the observed three modes. The mode P is nothing but the Zeeman transition between sublevels in $S = 1/2$ and $S = 3/2$ entities, the mode G the direct excitation of $S = 1/2$ entity which has the energy gap of Δ, and the mode F the coupled mode of the stable $S = 3/2$ entity and the less stable $S = 1/2$ entity, at least, at low temperature and finite field. For high temperature or low field, both $S = 3/2$ and $S = 1/2$ entities are likely to be changeable frequently and, thus, $M_{\text{A}} = M_{\text{B}}$, resulting in $g_{\text{eff}} = 0$. What is surprising is the fact that the F mode remains to be observed well above the saturation field $H_{\text{s}} = 15$ T at which the magnetization is saturated. It may suggests that the excited $S = 1/2$ entity can still survive dynamically even in the ferromagnetic saturated state due to quantum fluctuations. These results of magnetization and ESR studies are distinguishably different from those for a real $S = 3/2$ antiferromagnetic chain and we suggest that the difference in the excitation spectra of these systems which have different degree of internal freedom may be the origin of the interesting observation because the ferromagnetic intratrimer interaction is not infinitely strong.

Acknowledgements

This work was carried out under the Visiting Researcher's Program of IMR and partly supported by Grant-in-Aid for Scientific Research from the Ministry of Education, Science, Sports and Culture (Monbusho). SL and JPB were supported by Research Fellowship of the Japan Society for the Promotion Science (JSPS).

1) K. Okuda, H. Hata and M. Date: J. Phys. Soc. Jpn. **33** (1972) 1574.
2) D.C. Dender, D. Davidović, D.H. Reich and C. Broholm:

Phys. Rev. **B53** (1996) 2583.
3) D.C. Dender, P.R. Hammar, D.H. Reich, C. Broholm and G. Aeppli: Phys. Rev. Lett. **79** (1997) 1750.
4) M. Oshikawa and I. Affleck: Phys. Rev. Lett. **79** (1997) 2883.
5) I. Affleck and M. Oshikawa: Phys. Rev. **B60** (1999) 1038.
6) F.H.L. Essler and A.M. Tsvelik: Phys. Rev. **B57** (1998) 10592.
7) F.H.L. Essler: Phys. Rev. **B59** (1999) 14376.
8) M. Matsuura and Y. Ajiro: J. Phys. Soc. Jpn. **41** (1976) 44.
9) M. Oshima, K. Okuda and M. Date: J. Phys. Soc. Jpn. **44** (1978) 757.
10) M. Oshikawa and I. Affleck: Phys. Rev. Lett. **82** (1999) 5136.
11) Y. Ajiro, T. Asano, Y. Inagaki, J.P. Boucher, S. Luther, H. Nojiri and M. Motokawa: Proc. 22nd Int. Conf. Low Temperature Physics, Helsinki, 1999 (submitted to Physica B).
12) T. Asano, H. Nojiri, Y. Inagaki, J.P. Boucher, T. Sakon, Y. Ajiro and M. Motokawa: cond-mat 9911094.
13) F.D.M. Haldane: Phys. Rev. Lett. **50** (1983) 1153.
14) J.P. Renard, M. Verdaguer, L.P. Regnault, W.A.C. Erkelens, J. Rossar-Mignod and W.G. Stirling: Europhys. Lett. **3** (1987) 945.
15) K. Katsumata, H. Hori, T. Takeuchi, M. Date, A. Yamagishi and J.P. Renard: Phys. Rev. Lett. **63** (1989) 86.
16) Y. Ajiro, T. Goto, H. Kikuchi, T. Sakakibara and T. Inami: Phys. Rev. Lett. **63** (1989) 1424.
17) M. Date amd K. Kindo: Phys. Rev. Lett. **65** (1990) 1659.
18) W. Lu, J. Tuchendler, M. von Ortenberg and J.P. Renard: Phys. Rev. Lett. **67** (1991) 3716.
19) W. Palme, H. Kriegelstein, B. Lüthi, T.M. Brill, T. Yoshida and M. Date: Int. J. Mod. Phys. **B7** (1992) 1016.
20) L.C. Brunel, T.M. Brill, I. Zaliznyak, J.P. Boucher and J.P. Renard: Phys. Rev. Lett. **69** (1992) 1699.
21) T. Sakai and H. Shiba: J. Phys. Soc. Jpn. **63** (1994) 867.
22) P.M. Mitra and B.I. Halperin: Phys. Rev. Lett. **72** (1994) 912.
23) M. Sieling, U. Löw, B. Wolf, S. Schimidt, S. Zvyagin and B. Lüthi: cond-mat 9906273.
24) T. Takeuchi, T. Yoshida, K. Inoue, M. Yamashita, T. Kumada, K. Kindo, S. Merah, M. Verdaguer and J.P. Renard: J. Magn. Magn. Mater. **140-144** (1995) 1633.
25) A.M. Tsvelik: Phys. Rev. **B42** (1990) 10499.
26) Y. Ajiro, T. Asano, T. Inami, H. Aruga Katori and T. Goto: J. Phys. Soc. Jpn. **63** (1994) 859.
27) Ferromagnetic Resonance, ed. S.V. Vonsovskii (Pergomon Press, 1966), Chap.5, p.266.
28) K. Hida: J. Phys. Soc. Jpn. **63** (1994) 2359.